Novel Finishing Process Development for Precision Complex-Shaped Hemispherical Shell by Bulk Plasma Processing

D. Sam Dayala Dev, Enni Krishna and Manas Das

Abstract It is not uncommon that inertial sensor technology demands 'zero' surface and subsurface defects on sensing element microstructures, which are polished to very fine surface finish. Non-contact type unconventional finishing techniques are being developed to augment or replace chemo-mechanical polishing (CMP) technique for finishing such microstructures to remove subsurface damage. The aim of this study is to develop an atomistic material removal mechanism by chemical vaporization process. The novelty of this process is combining the merits of low-pressure plasma etching by ion such as isotropic material removal on all the surfaces simultaneously and merits of atmospheric plasma process such as chemical vaporization rather than physical bombardment by ions. This achieves defect-free extremely fine-polished surfaces. A finite element based Comsol® software package is used to model dielectric barrier excited RF discharge for helium and oxygen gas as processing gas and reactive gas, respectively. The gas composition, pressure, electrode configurations and power of RF excitation are studied with respect to oxygen radical formation and their uniformity of distribution in the chamber. Accordingly, plasma chamber is designed and built with Zerodur material with an optical window to achieve a deterministic process, which is capable of simultaneously polishing entire complex 3D surfaces including cavities where no tool or beam can reach. Plasma is established with helium as processing gas and oxygen and SF_6 are used as reactive gases at medium pressure of 20 mbar. The atomic emission spectroscopy is used to monitor the various oxidation states of silica and established correlation with respect to material removal rate and oxidation states of

D. S. D. Dev · E. Krishna
ISRO Inertial Systems Unit, Indian Space Research Organisation,
Thiruvananthapuram 695013, India
e-mail: samddev@gmail.com

E. Krishna
e-mail: kris.chem99@gmail.com

M. Das (✉)
Department of Mechanical Engineering, Indian Institute of Technology Guwahati,
Guwahati 781039, Assam, India
e-mail: manasdas@iitg.ernet.in

313

silica Si II and Si III. Fine-tuning of these parameters is done while polishing hemispherical shell based on atomic emission spectroscopy observations and established process with material removal rate of 0.008 mm^3/min. After repeated polishing cycles with cumulative 48 h of material removal, surface roughness (Ra) of 3.6 nm is achieved from as-machined shell of Ra = 903 nm.

Keywords Nanofinishing · Plasma polishing · Atomic emission spectroscopy Fused silica polishing

1 Introduction

The state-of-the-art inertial sensors demand on sensing microstructures, ultra-fine-surface finish with 'zero' surface or subsurface damage (SSD). Mostly, these microstructures of complex surfaces are realized in silica or fused silica materials. Fused silica has been used heavily in laser systems and optical systems which demand very high precision and complex shape. The most challenging task in optical component fabrication is achieving surface accuracy and surface finish. The need for shape accuracy and extreme surface finish is to be accomplished at the same time which demands innovative process for finishing optical glasses. The material processing technology has advanced to such an extent that 3D homogeneous fused silica is readily available with impurities limited to tens of parts per billion (ppb). Hence, the bulk material is not limiting the performance of the microstructures but the surface does. When the surface becomes thinner and thinner, zero surface and subsurface damage can totally modify the performance of these components. Therefore, the major challenge is to regain the bulk material properties on the surface to atomistic level while ensuring zero defects on the surface and subsurface. The normal line of manufacture of these brittle materials is through machining using diamond-coated milling cutter with/without ultrasonic assistance and further wet etching of the surface to eliminate all cracks and defects.

Wet etching invariably degrades the topography significantly while removing microcracks. Microcracks/bond strain gets removed but surface topography changes as shown in Fig. 1. As surface topography and surface finish get poor and subsurface defects are not completely removed, precision grinding is adopted to correct the topography and surface finish before resorting to conventional polishing technique such as chemo-mechanical polishing (CMP). Optical industries are able to achieve sub-nanometer surface finish with variance of CMP process.

In CMP process, apart from the chemical effect of the slurry on the surface, each abrasive makes a brittle machining for material removal. By the very nature of the

Fig. 1 Schematic of **a** machined surface, and **b** wet-etched surface
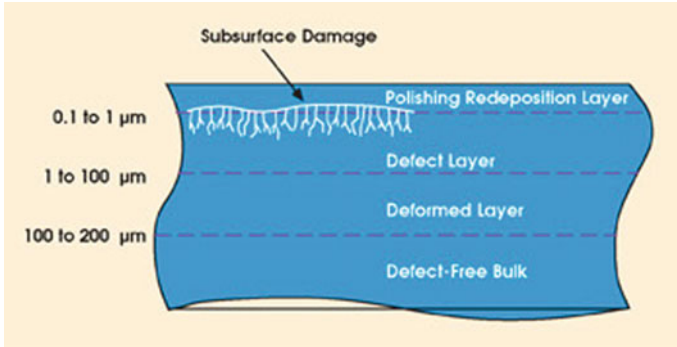
Fig. 2 Typical surface and subsurface defects occur in CMP process. With permission from Shena et al. (2005), copyright (2005) Elsevier

CMP process, the surface defects are submerged and redeposited layer forms which is chemical and mechanical property wise distinctly different from the bulk material. Also, these processes are not deterministic resulting in poor and inconsistent yield hiking the cost of these components. Typical surface and subsurface defects occur in CMP process as shown in Fig. 2. Therefore, processes such as magnetorheological finishing (MRF), elastic emission machining (EEM), etc., are developed as alternate finishing methods with least contact forces. Even though MRF is able to achieve very high surface finish with low SSD, it does not fully eliminate. Their applicability in finishing complex shape is very limited. Therefore, a non-contact type alternate line of finishing for glass or brittle components like plasma polishing is conceived in the present work, which is capable of atom-by-atom material removal from the surface at different material removal rates to replace wet etching and fine polishing processes.

1.1 Plasma Polishing

The plasma is known as a wide variety of macroscopically neutral substance having many interacting free electrons and ionized atom or molecules. In other words, plasma, which is called the fourth state of matter, is a partially ionized gas having same number of +Ve and −Ve particles. Ion is having positive charge and it is a molecule or atom of gas with a removed electron. Radical is a neutral particle (atom or molecule) that exists in a state of incomplete chemical bonding, and therefore it is chemically reactive. It is generated due to the fracture of a gas molecule by a high-energy electron collision. Equation (1) shows the oxygen radical ($\dot{o}$) formation.

Table 1 Plasma species for neutral molecules of density 10×10^{16}/cm^3

Radicals	10×10^{14}/cm^3
Electrons	10×10^{8}/cm^3
Positive ions	10×10^{8}/cm^3

Table 2 Plasma material removal mechanism spectrum

Decreasing pressure	Plasma characteristics	Increasing energy
<0.1 mbar	Physical (sputtering) momentum transfer directional etching	High energy and surface damage is high
0.2 mbar	Reactive ion etching physical and chemical variable anisotropy	Low energy
0.5 mbar	Chemical plasma etching, fast and isotropic material removal	
1–100 mbar	*Cold chemical plasma, bulk acting and isotropic material removal*	*Low-energy cold plasma model assumes zero plasma temperature*
1 bar	Atmospheric pressure plasma, cold chemical isotropic jet plasma (small aperture)	Very low energy, high surface integrity

$$O_2 + e^- \longrightarrow 2\,\dot{O} \tag{1}$$

There can be different forms of O_2 radicals such as O_2a1d, O_2b1s, O1d and O1s depending on the orbital position of the colliding electron. A typical plasma for a given neutral molecule of density 10×10^{16}/cm^3 contains typically the following species as shown in Table 1.

Therefore, more number of radicals (million times) than electrons or ions are available in the plasma. Radicals are formed more easily and also their lifetime is higher than electrons or ions. Ions do not etch or remove material. Ions affect the process by energetic (physical) bombardment on the surface, influencing the chemical process of atom-by-atom material removal. Radicals take part in dry etching or material removal process. Another property of radicals is their chemical activeness. Also, radicals react with the workpiece surface and volatile products are generated. Table 2 shows the wide spectrum of plasma material removal mechanisms for wide range of plasma gas pressure. The medium pressure of 1–100 mbar has the unique feature of being cold chemical plasma with a capability to act on the bulk of the specimen resulting in isotropic material removal. Table 3 lists the merits and demerits of existing low pressure and atmospheric plasma processing techniques with respect to the proposed medium-pressure plasma process. The generation of uniformly distributed plasma in a suitably designed chamber is possible with medium-pressure plasma process.

Also, in situ passivation and cleaning can be carried out on the specimen. All surfaces of 3D complex objects can be simultaneously and uniformly treated

Table 3 Plasma pressure versus polishing application

Applications and properties	Low-pressure plasma		Medium-pressure plasma		Atmospheric plasma	
	Advantages	Disadvantages	Advantages	Disadvantages	Advantages	Disadvantages
Plasma generation	Uniformly distributed plasma inside the chamber	Complex vacuum technology is required	*Plasma is distributed uniformly within plasma chamber*	*Complex vacuum and flow control is required*	Plasma treatment is possible directly even at the conveyor belt. No vacuum is necessary	The treatable area is limited to approximately 8–12 mm at a given time
3D objects	All items in the plasma chamber are treated simultaneously. Also, cavities can be treated from inside	None known	*All surfaces can be treated uniformly and simultaneously. Also, cavities can be treated from inside wide aperture*	*Establishing isotropic chemically reactive plasma is a challenge. Custom designed cavity may be required*	Local surface treatment is possible	Complex robotic technology is necessary. Treatment of surfaces with deep grooves is limited. Small aperture process
Surface integrity and surface finish of optics	Limited application	Due to anisotropy polishing cannot be done	*Very good as it is non-contact chemical reactive plasma*	*Only incremental surface finish improvement*	Surface integrity and surface finish improved	Very small area only can be covered

provided the shape, size and configuration of the plasma chamber and electrodes are suitably designed.

Plasma can be generated by either high DC voltage excitation or capacitive coupled radio frequency (CCRFD) excitation. CCRFD consists of two typically plane parallel electrodes of either same or different surface areas. The electrodes are placed inside the vacuum chamber in direct contact with the plasma or isolated from the plasma by a dielectric medium. If the electrode is behind a dielectric barrier, then it is called 'Dielectric barrier RF excitation'. Generally, the chamber is grounded. One electrode is joined to an RF generator via an impedance matching network and another electrode is connected to an RF high voltage waveform.

Due to difference between electron mass (m_e) and ion mass (m_i) ($m_i/m_e \gg 1$), the ion inertia is much higher than the electron inertia. Therefore, electrons have much higher energies than ions, and electrons will be lost in the walls quickly, if the plasma gets in contact with the boundary wall. As a consequence, a sheath of positive space charge will develop adjacent to the wall. In the sheath, an electric field accelerates ions towards the wall and repels electrons confining them in the discharge. In the sheath, quasi-neutrality is violated. In the quasi-neutral bulk, an ambipolar field coupled ion and electron diffusion. Depending on the choice of electrode surface area (chamber geometry) electrode gap, applied voltage waveforms, gas mixture, pressure and power, a variety of capacitively coupled discharges can be generated. Each type provides unique features useful for particular application. The gas mixture and pressure play the major role in defining the plasma characteristics. The choice of processing gas is essential for chemical processes in the plasma itself and at surfaces in contact with the plasma. Depending on the gas, the discharge might be electropositive or electronegative. Capacitive coupled dielectric barrier RF discharges can be operated at low pressure to less than 10^{-2} mbar for an isotropic etching process or at a high pressure, e.g. atmospheric pressure plasma jets. High-pressure micro-discharges can provide high radical density which is essential for material removal.

In the present study, a low power medium-pressure 'cold' plasma atomistic finishing process is conceived to achieve isotropic polishing of complex 3D surfaces concurrently including inside surfaces where no tool or beam can reach.

1.2 Literature Survey

The literate survey on plasma-based polishing methods done by different researchers is given below. Optical media is polished by the Gerhard et al. using dielectric barrier discharge gas plasma (DBDG) at atmospheric pressure (Gerhard et al. 2013). They achieved approximately 20% reduction in surface roughness along with 80% improvement in waviness with increased surface energy on optical materials including fused silica. The material removal is explained by ion bombardment and de-excitation of argon species. It is explained that the plasma discharge causes high electric field strength at roughness peaks. Hence, the waviness

improves distinctly. Wang et al. studied the surface changes in terms of surface modulus and hardness using atmospheric pressure plasma polishing (APPP) and they demonstrated improved surface mechanical properties (Wang et al. 2011). They reported that there is a decrease in surface residual stresses as the deformed layer is removed atom by atom from the surface. Jin et al. investigated the impacting factors on the surface roughness of Zerodur material by atmospheric pressure plasma jet (APPJ) polishing using He, O_2 and SF_6 (Jin 2010). Yao et al. (2010) reported the chemical machining of Zerodur material using APPJ. Wang et al. (2011) reported a novel non-thermal APPP for polishing SiC optics. Reactive gas such as CF_4 was introduced into the plasma area to react with the molecules at the surface of the SiC optics. Wang et al. (2009) developed highly stable SF_6 and Ar/O_2 capacitive coupled RF discharged method. Atmospheric pressure plasma with different working gases has been successfully developed to achieve sub-nanometer surface finish without surface damage but on a small aperture/area on the workpiece. However, this process is not suitable for bulk polishing of complex-shaped or freeform surfaces and inaccessible areas in precision microstructures. Inside surfaces, where the plasma torch cannot reach, atmospheric plasma fails to be useful.

Liu et al. (2009) reported the low-pressure plasma polishing process in the range of 10^{-2}–0.5 mbar and it is capable of reducing/removing the subsurface damage on complex freeform surface. However, there is no appreciable improvement in the surface finish but surface integrity is enhanced in terms of surface residual stresses. Enough literature is available with respect to the low-pressure plasma etching with available custom-built industrial equipment and machines.

Wang et al. (2006) developed a novel non-thermal atmospheric pressure plasma for polishing SiC optics. Reactive gas such as CF_4 was introduced into the plasma area to react with the molecules at the surface of the SiC optics. As the interaction is a pure chemical process, the material removal is at the atomic and no surface damage is caused.

Dev et al. (2016) targeted to develop an atomistic finishing process combining the best of low-pressure plasma processing capabilities such as removal of surface and subsurface damaged layer simultaneously on all the surfaces of the component and atmospheric pressure plasma polishing capabilities such as fine polishing and isotropic material removal. The process is novel from the fact that it is capable of polishing simultaneously entire complex 3D surfaces including cavities where no tool or beam can reach.

There is numerous application of freeform optics in reflective, refractive and diffractive optical system which demand finishing multiple surfaces on a single microstructure or inside surfaces which cannot be accessed by any tool or jets (either abrasive jets or plasma jets). Freeform optics are designed to improve the optical performance by removing the optical aberrations, improving the performance level many folds. Nanofinishing of such freeform surfaces in optics and sensor microstructure realized from glass or glass-like materials is thought to be not achievable. However, newer and innovative processes are being developed for nanofinishing such components.

Low-pressure plasma is known for the high MRR, and anisotropic plasma machining has been effectively used for such application. As the pressure of the plasma is increased, the isotropic property is gained and the energy level keeps coming down. The atmospheric pressure plasma is a low-energy isotropic plasma polisher. Inside surfaces or where the plasma torch cannot reach, atmospheric plasma fails to be useful.

Enough literature is available with respect to low-pressure plasma etching/polishing and custom-built industrial equipment and machine are also being available. Also, a very active research is being carried out in atmospheric pressure plasma polishing for wider applications. However, there is no literature available in medium-pressure isotropic cold plasma polishing.

1.3 Motivation of the Present Work

The navigation grades inertial sensors such as gyros and accelerometers have sensing microstructures which demand high order of precision and surface finishing to enhance the surface integrity which has direct impact on the performance of the sensors. The motivation behind the present work is to develop a finishing process to enhance the surface integrity of the polished surface up to 2–3 Å. Variants of conventional chemo-mechanical polishing are adopted to achieve such surface finish but the yield has been poor as the processes are not deterministic to achieve 'Zero defects' in critical locations. Most of such optics passes through stringent inspection with white light. However, when inspected in laser light, the subsurface damage (SSD) shows up as spots of light scattering resulting in rejection. The typical yield in laser light inspection is of the order of 10–12% and is primarily due to the contact mode of polishing which results in molecular level distortions/strained bonds. The laser gyro components and hemispherical resonator gyro (HRG) components are shown in Figs. 3 and 4, respectively.
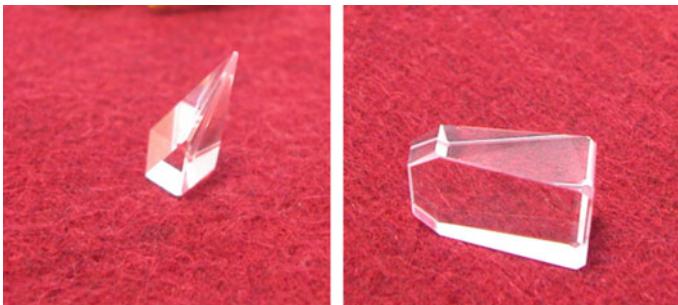
Fig. 3 ISRO laser gyro components

Fig. 4 Hemispherical
resonator gyro
(HRG) components

Hence, a non-contact type surface finishing method in which the surface integrity is enhanced while maintaining or improving the surface finish is studied. The expected surface material removal is limited to 10–1000 nm. Another application is where the microstructures display complex and/or freeform surfaces which needs to be polished to sub-nanometer finish from as-machined or ground workpiece while maintaining very high surface integrity level with respect to subsurface damage and residual stresses. Added to above requirements, the process shall not damage/degrade the topography and geometrical tolerances. The scope of present activity is focussed towards the development of a non-conventional non-contact type surface finishing process applicable to glass, fused silica and similar brittle materials.

2 Comsol Simulation

The primary aim is to identify the electron density and uniformity of distribution and O_2 radical's distribution with respect to the shape of the chamber, position and shape of the electrodes. Study the electron temperature to confirm the electron temperature is benign and 'cold' plasma conditions are maintained. Also, the Comsol model is validated with experimental atomic spectroscopy results and analytical model. The following objectives are identified:

- Investigate the effect of mixture of helium and oxygen gas on the SiO_2 specimen inside the plasma chamber by varying the volume concentration and pressure.
- Study the effect of shape, size and position of specimen inside the plasma chamber.

Table 4 The main reactions occurring inside the plasma chamber

Electron impact reactions	Heavy species transport reactions	Surface reactions
e + He => e + He	$He^* + O_2 => O_2^+ + He + e$	$He^* => He$
e + He => e + He*	$He^+ + O_2 => O^+ + O + He$	$He^+ => He$
e + He => 2e + He$^+$	$He^+ + O_2 => O_2^+ + He$	$O_2^+ => O_2$
e + O$_2$ => 2e + O$_2^+$		$2O^+ => O_2$
e + O$_2$ => e + O$_2$a1d		
e + O$_2$a1d => e + O$_2$		
e + O$_2$ => e + O$_2$b1s		
e + O$_2$b1s => e + O$_2$		
e + O$_2$ => e + O + O		
e + O$_2$ => e + O + O1d		
e + O$_2$ => e + O + O1s		

- Also, design the shape, size and position of electrode outside the plasma chamber to get homogeneous distribution of reactive species and ions.

In the present case, a two-dimensional frequency transient study under microwave plasma (MWP) is used for simulation. Electric field is setup using out-of-plane vector considering the signal in transverse electric mode. Reduced electron transport properties are considered to account for the heavy species transport. The pressure and temperature of the plasma are taken as 25 mbar and 300 K, respectively, and are considered to be constant throughout the operation of the plasma. Plasma setup is made considering the plasma to be static. The different species used for current simulation are, in molecular state: He and O$_2$, ions: He$^+$, e, O, O$^+$, O$_2^+$, and radicals: O$_2$a1d, O$_2$b1s, O1d, O1s, He*. To study the plasma chemistry, the main reactions occurring inside the plasma chamber are shown in Table 4.

For each of the heavy species, the molecular weight, potential characteristic length and potential energy minimum are required to compute the correct diffusivity and mobility. The initial number density for electron is considered as $1 \times 10^{17}/m^3$. Considering the plasma to be neutral consisting of ions and electrons, the initial number density and initial mole fractions of different species (ions and electrons) are to be equal. Since the radicals (excited species) are formed at a later part during reaction, the initial mole fraction of the radicals is considered very small (negligible), i.e. $1–5 \times 10^{-8}$.

2.1 Computational Domain and Boundary Conditions

The geometry of the two-dimensional computational domain as shown in Fig. 5 is prepared similar to the proposed experimental setup. The cross-sectional area of the setup is prepared into three domains, i.e. dielectric, plasma and electrode (Fig. 5).
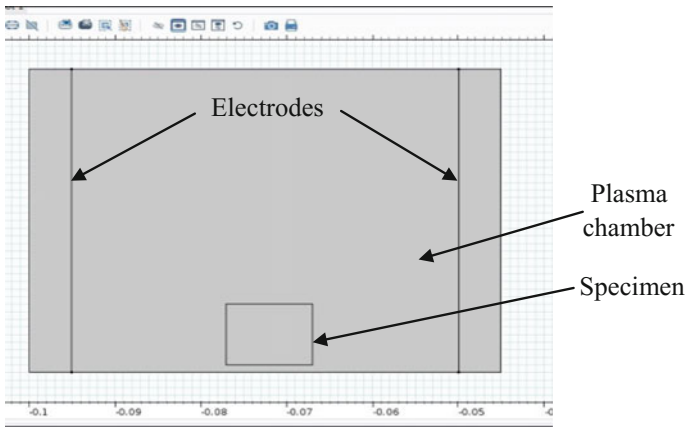
**Fig. 5** 2D computational domain of the plasma chamber

The electrodes are placed at the extreme boundaries on both left and right sides of the setup. The setup dimensions considered are (55×40) mm^2, and the thickness of the dielectric chamber is 5 mm. A specimen of SiO$_2$ (quartz) is taken at the bottom of the chamber. The dimension of the specimen is (10×8) mm^2. A physics-controlled mesh of finer nature is used to carry out the simulation. The mesh at the boundaries is made finer to accommodate the collision of the charged particles. Free triangular mesh is considered.

The four boundaries of the plasma chamber are considered as the four walls in the model containing the plasma within the domain. The four boundaries of the chamber are grounded so as the surface reactions to take place at the boundaries. The plasma is excited using an RF frequency as a port applied to one electrode while another electrode opposite to the first electrode is grounded. Square-wave RF signal is used for exciting the plasma, and the power level considered is 40 W.

## 2.2 Comsol Simulation Results and Discussion

It is a transient analysis and steady state is reached before one second. The plasma condition at 1 s is taken for comparison study for all cases. The electron density and O$_2$ radials such as O1s and O$_2$b1s are studied. In Fig. 6a, b, the electron density is shown without and with the specimen, respectively, inside the plasma chamber. The electron density varies from 1×10^{16} to 6×10^{16} 1/m^3 for both the cases. However, the distribution profile is altered while the specimen is placed inside the chamber. Hence, it is understood that the shape and position of the fused silica influence the distribution of electron density inside the polishing chamber.

After that a cylindrical fused silica specimen of varying sizes with respect to the plasma chamber is placed inside the plasma chamber to understand the effect of

(a)

(b)
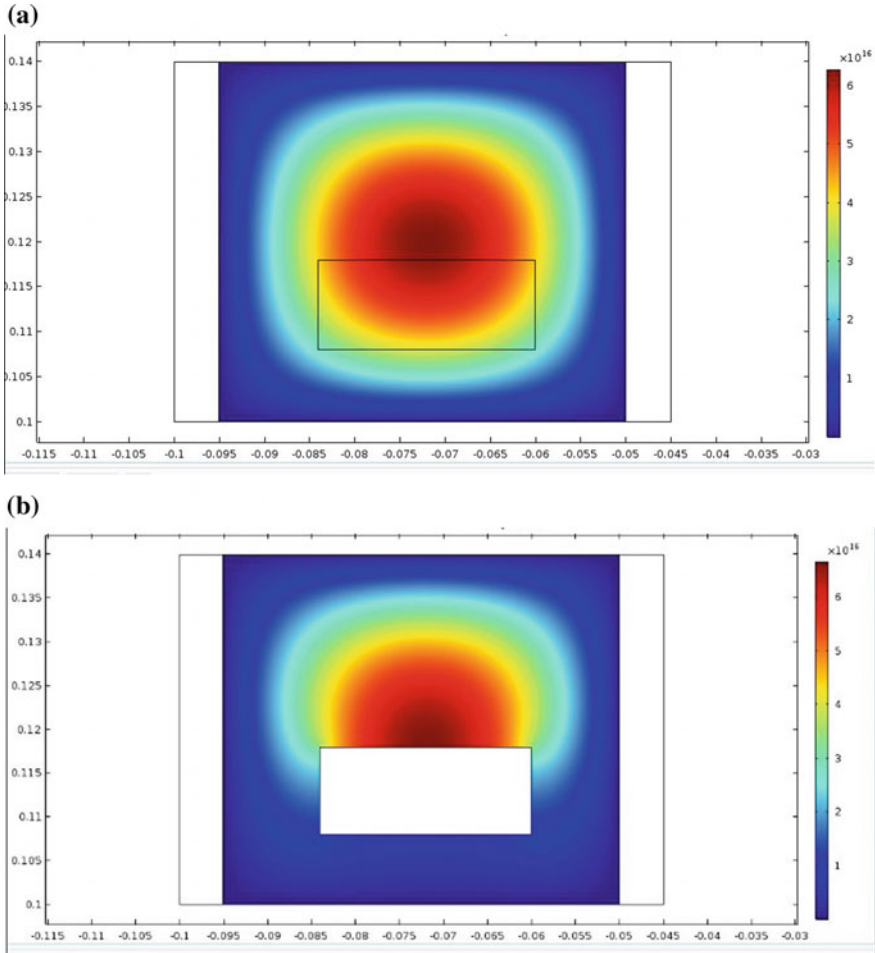
Fig. 6 Electron density **a** without, and **b** with specimen inside plasma chamber

specimen size inside the plasma chamber (Fig. 7). In Fig. 7a–c, the specimen sizes are approximately three-fourth, half and one-fourth of the chamber size, respectively. As shown in Fig. 7, the electron density distribution is not uniform when the specimen is large (Fig. 7a) compared to the cross section of the chamber. In other words, when the free volume is less, the electron density is lower and non-uniform. As the specimen size reduces, i.e. free volume of the chamber increases, the uniformity of the electron density distribution improves distinctly and electron density also increases. The same is true for the distribution of O_2 radials such as O1s and O_2b1s (results not shown here). However, there is no variation in the number density of radicals irrespective of the size of the specimen.
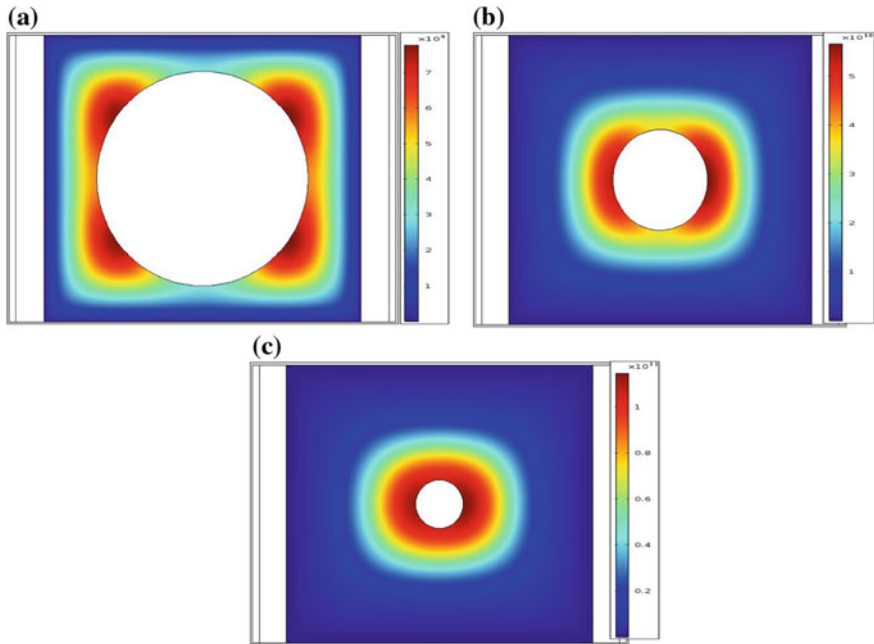
Fig. 7 Electron density when specimen sizes are **a** three-fourth, **b** half and **c** one-fourth of chamber size

From Fig. 8, it is observed that as the O_2% increases, the number density of O1s radicals increase. However, the distribution of O1s radical is unsymmetrical with respect to the specimen up to at 1% and symmetrical at 2% and it loses its symmetrical distribution on further increase of O_2%. Therefore, 2% O_2 composition may be optimum for processing fused silica components.

Based on the Comsol simulation results, the plasma chamber along with electrodes is modified to suit target specimen of hemispherical shell made of fused silica. Figure 9a shows the plasma chamber with two parallel electrodes with respect to the position of the HRG shell. Figure 9b shows the same plasma chamber with four-sided electrodes. The corresponding distribution of O_2b1s radicals is shown in Fig. 10. The number density of O_2b1s radicals is more by 18% for four-sided electrode configuration than electrode placed at top and bottom. Hence, more material removal is expected while polishing with four-sided electrodes.
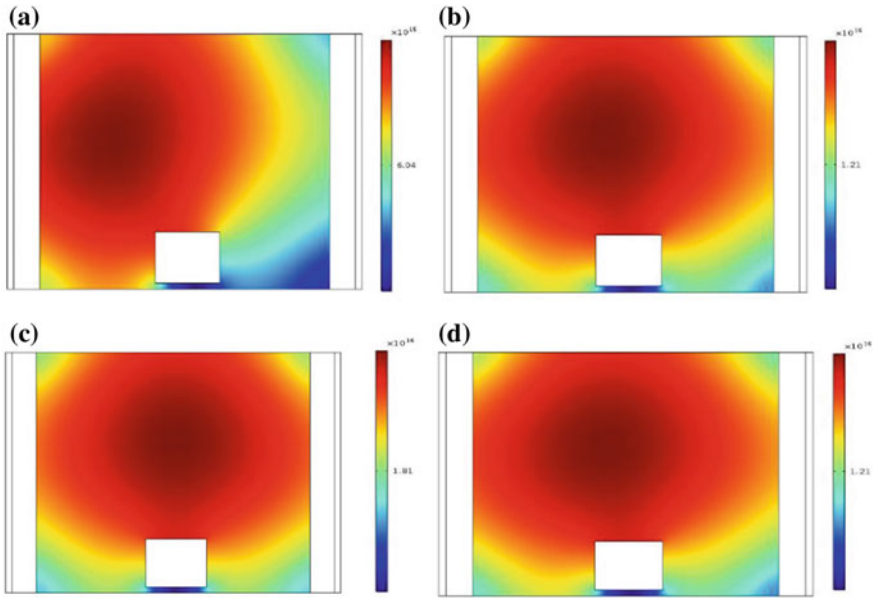
Fig. 8 Number density variation of O1s radical with increasing O_2 concentration (%) **a** 1%, **b** 1.5%, **c** 2%, **d** 5%
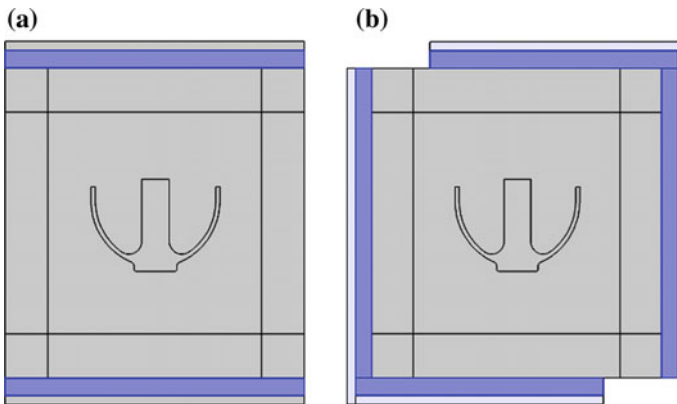
Fig. 9 2D computational domain of the plasma chamber with **a** two parallel electrodes at top and bottom, and **b** four-sided electrodes
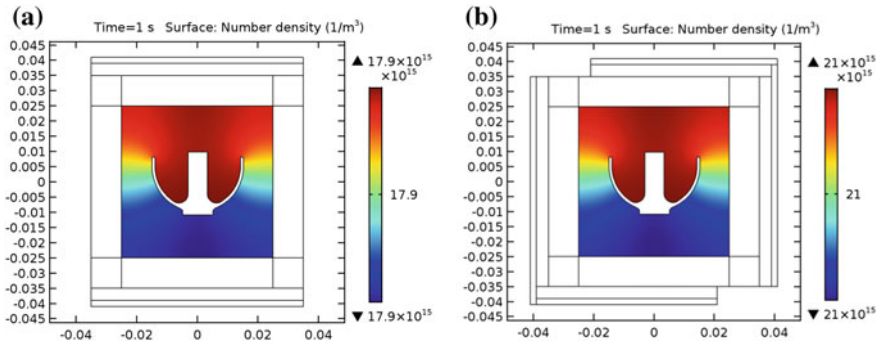
Fig. 10 Distribution of number density of O_2b1s radicals inside plasma chamber with **a** two parallel electrodes at top and bottom, and **b** four-sided electrodes

3 Design and Development of Experimental Setup

The configuration of the experimental setup developed based on simulation results of plasma analysis using finite element based software package Comsol®. The basic requirements of the present plasma polishing set up are as follows:

- The setup should have hermetically sealed chamber to maintain required vacuum/low pressure.
- The chamber should have interface to vacuum system and multiple gas feed lines for processing and reactive gases.
- The body of the plasma chamber shall act as a dielectric for RF excitations for the plasma with electrode placed outside the chamber.
- The chamber shall have optically transparent window for wavelengths 200–1200 nm in order to characterize the plasma by optical emission spectroscopy.

Based on above requirements, the plasma chamber is fabricated using Zerodur material body with fused silica cap as shown in Fig. 11a. The fused silica lid plate is optically transparent in the required wavelength. The chamber is connected to the vacuum system and gas feed lines through glass tubes. The glass tube feed lines are connected to the chambers by glass blowing technique. The schematic diagram of the experimental setup is shown in Fig. 11b.

3.1 Optical Emission Spectroscopy

It is required to interpret the mechanism of material removal, i.e. the generation of reactive species and generation reacted products with time during plasma polishing. The optical emission spectroscopy is a very useful tool to continuously monitor the relative spectroscopy densities of plasma species in the excited electronic states.
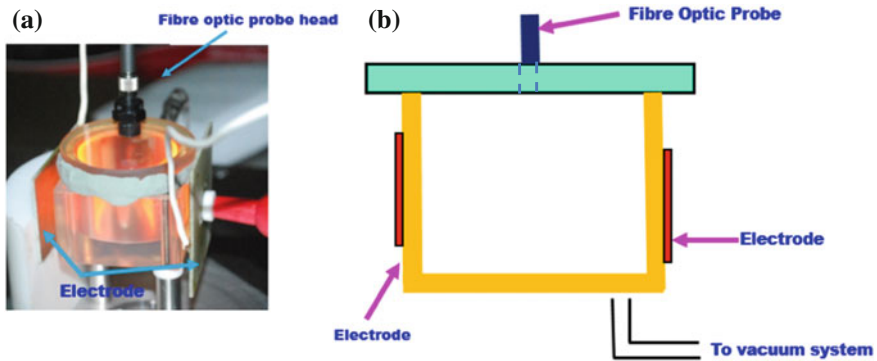
Fig. 11 **a** Actual photograph, and **b** schematic diagram of plasma polishing experimental setup

In a plasma, the excited atoms obtain enough energy, so that outer shell electron will transit to an excited state with higher energy. Since it is unstable in that state, it settles to a low energy level emitting electromagnetic radiation giving rise to an optical emission spectrum. The wavelength and energy change of the spectrum are related as

$$\lambda = hc/\Delta E \tag{2}$$

where ΔE is the energy difference between two levels of atomic state, λ is the wavelength of emission, h is the Plank's constant, and c is the speed of light. The transition and hence relative densities of the species are identified based on measured spectral line (λ) in the plasma and National Institute of Standards and Technology (NIST) atomic spectra database. The fibre optic probe head of atomic emission spectrometer (Ava spec ULS 2048 from Avantes Inc. Netherland) is placed at the fused silica cap of the experimental setup. The optical emission spectroscopy and its probe positioned at plasma chamber are shown in Fig. 12a, b, respectively.

The plasma chamber shall enable generation of reactive species uniformly covering the components to be polished. The preliminary experimental setup was
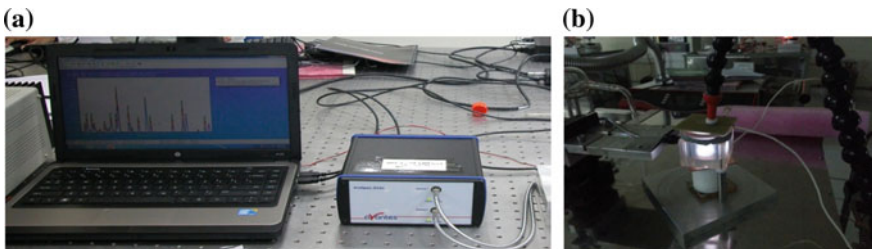
Fig. 12 **a** Optical emission spectroscopy set up, **b** its probe positioned at plasma chamber

Table 5 Specification of plasma processing setup

Discharge volume	Gap between the electrodes	Discharge frequency	Substrate used	Processing and reactive gases
30 cc ($D = 40$ mm, $H = 25$ mm)	50 mm	40.68 MHz	Fused silica	He, Ne and O_2 and SF_6

targeted to finish components of size ranging between 5 and 30 mm. The schematic diagram of experimental setup is shown in Fig. 12b. For a plasma polishing process to happen, generation of the reactive species and their adsorption at the component surface is essential. Then, the chemical reaction of the radicals (reactive species) and physical bombardment of the ions results in material removal atom by atom. The reacted volatile product diffuses away from the surface to be flushed out. Hence, it is very important of higher generation of the reactive species and their homogeneity over the component (all over the surfaces) for uniform material removal from complex freeform surfaces. The medium range pressure level is chosen to eliminate the damaging effects of ion impingement. In addition, RF excitation is used to limit electron heating while allowing chemical interaction of free radicals with surface atoms of workpiece. The RF excitation frequency of 40.68 MHz is chosen to minimize ion bombardment. The exact shape and size of the electrodes are configured based on information from simulation study using Comsol®. The specification of plasma processing setup is given in Table 5.

3.2 Experimental Procedure

The first step followed is to characterize the processing gas and reactive gas mixtures and fine-tune the gas mixture ratio and pressure. Preliminary experiments are conducted by characterizing the plasma with He, Ne and O_2 as processing gases, and O_2 and SF_6 as reactive gases at different pressures, different gas mixture ratios and RF excitation power level. Based on the observed experimental results by the optical emission spectroscopy, the selected gases are He as processing gas, oxygen as catalyst cum radical donor, and SF_6 as radical/ion donor (Liu 2009).

### 3.2.1 Characterization of Plasma for Reactive Gases

Reactive radicals such as fluorine are to be present for sustained material removal by plasma. The chemically active neutral substances (i.e. free radicals) of the F* which is dissociated from SF_6 will react with silica to form volatile products as per the following equation:

Table 6 Observed silica ion, fluorine and SiF transition lines

Element	Line (nm)	I-rel	Energy Ev Lower–Upper	Transition Lower–Upper	Quantum no Lower–Upper
II	450.7152	1996	33.04–35.79	3d′ 3P0–4f′ 2[5/2]	2–3
F III	449.5077	7763	55.12–7.88	4f 2 (Jin 2010) 0–5 g 2 (Wang et al. 2011)	9/2–11/2
SiF	449.58	600	0.00–2.84	X2Pi–A2Sig+	3–3
Si III	482.897	12303	25.99–28.55	4f 3F0–5 g 3G	4–5
Si IV	480.1437	132	39.08–41.67	6f 2F0–8d 2D	7/2–5/2
Si II	519.286	2512	16.36–18.75	4p′ 4D–4d′ 4F	5/2–7/2
Si II	518.525	1259	16.35–18.74	4p′ 4D–4d′ 4F	3/2–5/2
Si II	518.19	1000	16.34–18.73	4p′ 4D–4d′ 4F	1/2–3/2

$$SiO_2 + 4F^* \longrightarrow SiF_4 \uparrow \, + O_2 \uparrow \tag{3}$$
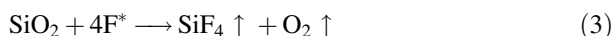
Another possible chemical reaction, i.e. the positive F^+ ion, reacts with the substrate to form volatile products as per the following equation:

$$4F^+ + SiO_2 + 4e^- \longrightarrow SiF_4 \uparrow \, + O_2 \uparrow \tag{4}$$
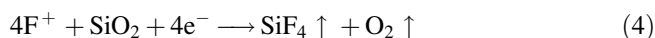
Accordingly, SF_6 gas is introduced as reactive gas. With this chemistry of gases, the silica and fluorine peaks are predominant between 440 and 520 nm as shown in Table 6 from NIST database.

Plasma processing is done at 20 mbar pressure and 40 W power, where uniform plasma distribution is obtained. Experiments are carried out to study the effect of SF_6/O_2 ratio on material removal rate (MRR) of the shell and it is shown in Fig. 13. MRR is the highest when the ratio of SF_6/O_2 is 2. The rate of material removal is 1.1 mg/h. The mean material removal rate of 0.008 mm^3/min is achieved for the optimized reactive gas mixture. The gas mixture selected after a series of experiments is He: 19.25 mbar, O_2: 0.25 mbar and SF_6: 0.5 mbar.

For further experiments, each cycle duration is fixed to 20 min and the chamber is evacuated to flush out the volatile products. After that the chamber is refilled for

Fig. 13 Weight loss versus ratio of SF_6/O_2
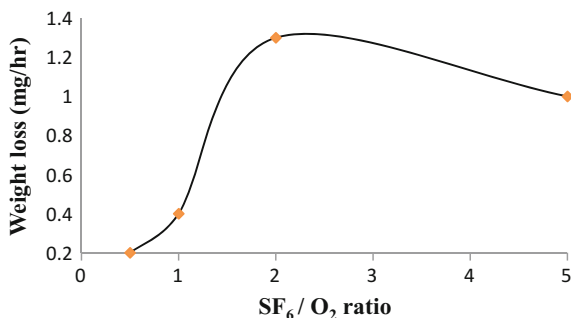
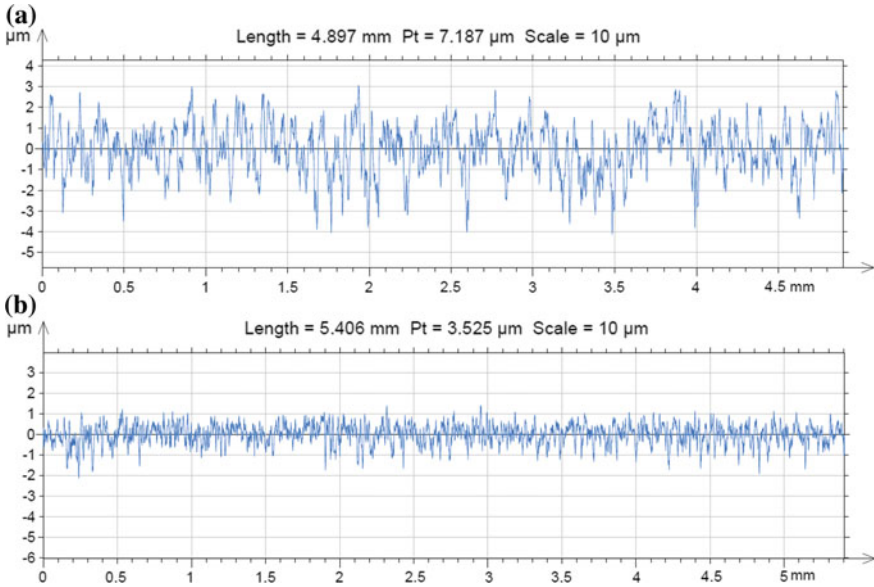**Fig. 14** Silicon ions and SiF transitions with time
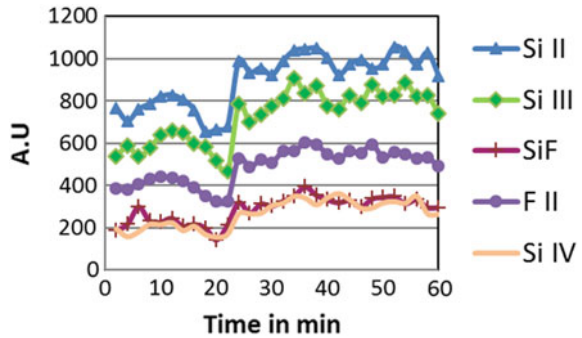
next cycle of experiments. Multiple such cycles are performed and the silicon ion and SiF transitions are plotted with time (Fig. 14). For a weight loss of 1.1 mg/h for the given specimen, the mean material removal rate is 0.01 mm^3/min. Compared to the MRR for atmospheric pressure plasma reported in the literature, the present MRR is low.

## 3.3 Initial Stage Polishing of Hemispherical Shell

Based on the parameters optimized during preliminary experimental study, plasma processing of fused quartz hemispherical shell is carried out. Different views of the shell as compared with Indian one rupee coin are shown in Fig. 15. After one level of plasma processing with three cycles of 20 min duration, the surface roughness profile is recorded as shown in Fig. 16b from its initial as-machined condition (Fig. 16a). When the number of cycles is further repeated, the MRR is reduced drastically. It is suspected that certain polymers are forming on the specimen surface and due to which MRR is reduced for further cycles. The surface residual stress or molecular level strained bonds are expected to be better with plasma-processed

Fig. 15 Fused silica shell (two different views)

(a)

μm

Length = 4.897 mm Pt = 7.187 μm Scale = 10 μm

(b)

μm

Length = 5.406 mm Pt = 3.525 μm Scale = 10 μm

Fig. 16 Surface profiles **a** as machined (Ra = 0.90 μm, Rz = 6.44 μm), **b** after three cycles of 20 min duration plasma polishing (Ra = 0.38 μm, Rz = 2.81 μm)

(a)   **(b)**
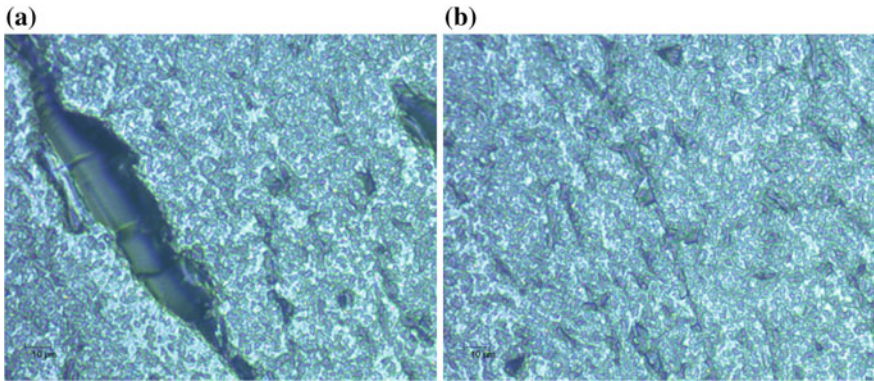
Fig. 17 AFM surface image **a** as machined, and **b** after three cycles of 20 min duration of plasma processing

surface. The surface finish is improved from 0.90 to 0.38 μm only. However, the surface cracks and damages are effectively removed from the plasma-processed surface as shown in atomic force micrograph (AFM) image (Fig. 17b) from the as-machined surface as shown in AFM image in Fig. 17a.

3.3.1 Fine Plasma Polishing of Hemispherical Shell

The shell is subjected to cumulative plasma polishing for 48 h and the product is shown in Fig. 18. After multiple sessions of plasma polishing cycles, the component is left with patches of opaque regions apart from transparent surface.

The surface finish is measured by non-contact Brooker contour GTK-A surface profilometer. The 3D surface roughness profile of the shell from areas having non-transparent patches and transparent region is shown in Fig. 19a, b, respectively. In Fig. 19b, the surface finish is improved to 3.6 nm from the shell's initial surface roughness value of 902 nm. It is also observed from Fig. 19a, i.e. from the areas of non-transparent patches, that the surface finish has improved to 32 nm and it is due to the presence of few fine digs, i.e. crater-like defects. These defects are primarily due to the ultrasonic-assisted brittle machining, i.e. milling operation adopted to shape the job from a cylindrical bar. Suitable process modification is required for further improvement of the shell surface. This gives confidence that medium-pressure plasma polishing is capable of polishing complex surface such as hemispherical shell.

Fig. 18 Hemispherical shell of fused silica after plasma polishing
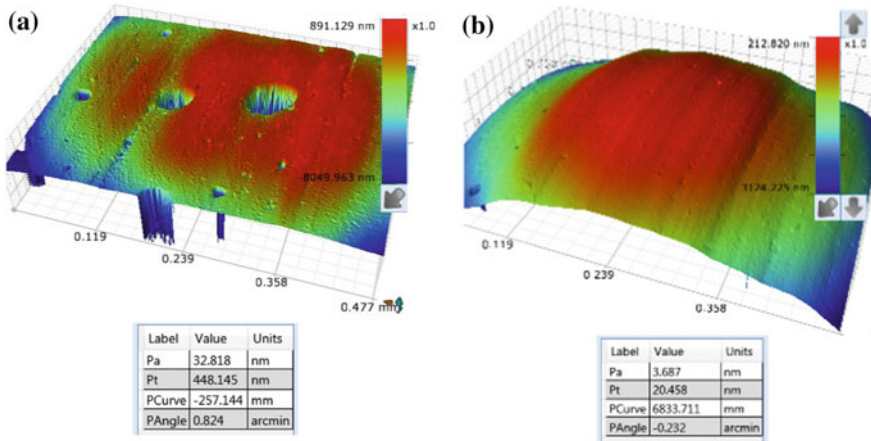
Fig. 19 3D contour surface profiles on curved shell (Fig. 18) surface **a** with defects (Pa = 0.0328 μm, Pt = 0.448 μm), and **b** on transparent surface (Pa = 0.0036 μm, Pz = 0.045 μm)

4 Conclusions

Comsol$^®$ finite element simulation of the plasma is used to analyse the distribution of the radicals inside the plasma chamber with and without specimens and for the ratio of free volume to the total available volume of the chamber for uniform distribution of radicals. The ratio of processing gas and reactive gas is identified for optimum distribution of radicals. In the presence of hemispherical shell component, the four-sided electrode provides higher density of radicals. The experimental setup is designed and built based on preliminary inputs from Comsol$^®$ analysis, and four-sided electrode is used for shell processing. The gas mixture is fine-tuned to get best MRR of 0.008 mm^3/min. The atomic emission spectroscopy is used to monitor the various oxidation states of silica and to establish correlation with respect to MRR and intensity of oxidation states of silica Si II and Si III. With initial plasma processing for one-hour duration, the surface finish is improved from Ra = 0.90 nm to Ra = 0.38 nm. The AFM images after pre- and post-plasma polishing confirms elimination of large cracks/indents. The plasma process could efficiently play the role of wet etching in removing the surface cracks and damages without degrading the surface topography. Cumulative plasma polishing of 48 h has resulted in surface finish of the order of 3.6 nm (Pa) in most of the locations. However, in the areas with patches, the surface roughness of 32.82 nm (Pa) is obtained which is attributed to the excessive damaged surface due to ultrasonic milling process adopted for shell shaping prior to polishing.

References

Dev, D.S.D., E. Krishna and M. Das. 2016. A Novel Plasma assisted atomistic surface finishing on freeform surfaces of fused silica. *International Journal of Precision Technology* 6: 262–276.

Gerhard, C., T. Weihs, A. Luca, and S. Wieneke. 2013. Polishing of optical media by dielectric barrier discharge inert gas plasma at atmospheric pressure. *Journal of the European Optical Society—Rapid Publications* 8: 13081–13085.

Jin, H.L., B. Wang and F.H. Zhang. 2010. Effect on surface roughness of zerodur material in atmospheric pressure plasma jet processing. *Proceedings of SPIE* 7655: 76552X 1–7.

Liu, W., D. Wang, M. Hu, Y. Wang, H. Liang and L. Hang. 2009. Roughness evaluation of fused silica plasma polishing. *Advanced optical Manufacturing Techniques-Proceeding of SPIE* 7282: 72822T 1–5.

Shena, J., S. Liuc, K. Yi, H. He, J. Shaoa, and Z. Fan. 2005. Subsurface damage in optical substrates. *Optik—International Journal for Light and Electron Optics* 116: 288–294.

Wang, B., J. Zhang, and S. Dong. 2006. Application of atmospheric pressure plasma in the ultrasmooth polishing of SiC optics. *Materials Science Forum* 532–533: 504–507.

Wang, B., J. Zhang, and S. Dong. 2009. New development of atmospheric pressure plasma polishing. *Chinese Optics Letters* 7: 537–538.

Wang, D., W. Liu, Y. Wu, L. Hang, H. Yu, and N. Jin. 2011. Material removal function of the capacitive coupled hollow cathode plasma source for plasma polishing. *Physics Procedia* 19: 408–411.

Yao, Y.X., B. Wang, J.H. Wang, H.L. Jin, Y.F. Zhang, and S. Dong. 2010. Chemical machining of Zerodur material with atmospheric pressure plasma jet. *CIRP Annals-Manufacturing Technology* 59: 337–340.